



Method of operating a GIS-based autopilot drone to inspect ultrahigh voltage power lines and its field tests

Joon-Young Park¹ | Seok-Tae Kim¹ | Jae-Kyung Lee¹ | Ji-Wan Ham¹ | Ki-Yong Oh²

¹Power Transmission Laboratory, KEPCO Research Institute, Korea Electric Power Corporation, Daejeon, Republic of Korea
²School of Energy System Engineering, Chung-Ang University, Seoul, Republic of Korea

Correspondence

Joon-Young Park, Power Transmission Laboratory, KEPCO Research Institute, Korea Electric Power Corporation, 105 Munji-Ro, Yuseong-Gu, Daejeon 34056, Republic of Korea.
Email: joonyoung.park@kepco.co.kr

Abstract

The drone-based inspection process on power transmission lines needs to be automated due to the large scale of power facilities and the limited line of sight available to drone pilots. Through the task environment analysis, however, it was found that the steel tower structure and energized AC power conductors may cause GPS signal distortion and magnetic interference with a drone's geomagnetic sensor, respectively. These factors could seriously affect the drone's autopilot flight, at worst leading to a crash. To enable drone inspections to be performed in a safe and efficient manner, this paper presents the entire process of operating an autopilot inspection drone on the basis of GPS and GIS information in a hazardous ultrahigh voltage environment, and its application results in the field. This process includes how to measure GPS co-ordinates of steel towers and how to generate an autopilot flight path. More specifically, the paper examines the potential problems that may occur when drones are applied to areas located in mountains and rivers where humans cannot inspect power lines due to a lack of accessibility, and proposes effective solutions to these practical issues.

KEY WORDS

autopilot flight, flight path planning, inspection drone, operation method, power transmission line

1 | INTRODUCTION

Most power transmission lines built in Korea are located in mountainous areas, meaning accessibility to the lines is very low, and live-line maintenance work is very dangerous due to high places and ultrahigh voltage. Therefore, overhead power line monitoring has been done by traditional monitoring methods like walk-around inspection and high magnification telescope-based inspection. However, these methods have been shown to have some limitations in that due to poor accessibility, it may take a considerable amount of time to reach a target location and it is often difficult to secure a clear view of the inspection target. Also, the shortage of skilled manpower in this field is getting worse in connection with the current social phenomenon of avoiding 3D jobs.

To deal with these issues and inspect power lines efficiently, various research works to adopt unmanned helicopters have been

carried out. Shandong Electric Power Research Institute in China developed an unmanned helicopter to inspect 220 kV transmission lines through video cameras and thermal imaging cameras (Wang et al., 2010; Wang, Han, Zhang, Wang, & Li, 2009). Deusto University in Spain has carried out the RELIFO research project together with IBERDROLA, a Spanish electric utility company (Larrauri, Sorrosal, & González, 2013). The goal of this project was to develop a new automatic system that could be operated in real time for overhead power lines inspection by an unmanned aerial vehicle.

In this context, drones have drawn global attention recently for inspecting electric facilities because of their easier control, flight safety, and wide availability compared to unmanned helicopters. Electric Power Research Institute (EPRI) in the U.S. has made evaluations on drone applicability for power line monitoring since 2014 (Unmanned Air Systems for Transmission Line Inspection,

2016; Unmanned Aircraft Systems for Power Line Inspection, 2015) and seven electric companies such as Commonwealth Edison and PPL Electric in the country have been approved by the U.S. Federal Aviation Administration to use drones to inspect their lines in 2015 (ComEd gets OK to deploy drones for power system inspections, 2015; PPL starts using drones to help inspect high-voltage lines, 2015). Power companies in Europe and Mexico are also performing transmission line inspection using drones (Luque-Vega, Castillo-Toledo, & Loukianov, 2014). In Korea Electric Power Corporation (KEPCO), Technical Diagnosis Department and regional offices have used drones equipped with optical zoom cameras and thermal imaging cameras to inspect electric poles and steel towers for power distribution lines since 2015 and were able to detect malfunctions and faults; Gyeongin Construction District Department and Gyeongnam Regional Office also developed an engineering method to replace helicopters they had used with drones so that they can easily carry out overhead power line stringing between steel towers.

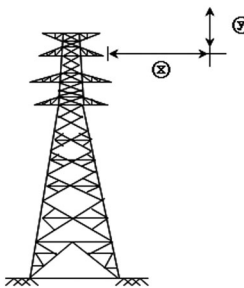
All drone-based inspections mentioned above were directly controlled by professional pilots with the naked eye, but still problems arose; steel towers are very tall and the span between them is pretty wide. Moreover, the process of controlling a rotary UAV under a 500-m span with a 250-m line of sight is prone to errors and hazards (On Airborne Inspections, 2014). For this reason, it would be very difficult to monitor the power lines with the manual remote control of drones. Attempts to overcome this limitation have included some research on vision-based line inspection (Han et al., 2018; Martinez, Sampedro, Chauhan, Collumeau, & Campoy, 2018; Nguyen, Jenssen, & Roverso, 2018; Ribeiro, Duarte, Ramos, & Mora-Camino, 2018). However, most of these works have focused on image-based diagnosis using deep learning, and vision-based drone control methods are not sufficiently mature to be used directly in industrial sites. Through on-site experiences, it was concluded that inspection drones should fly on autopilot along a planned path based on the geographic information and its related GPS co-ordinates due to the large scale of power transmission lines in terms of their height and span. This paper will deal with a GIS-based automatic drone inspection system for power transmission lines developed by us, its operation and field tests.

2 | TASK ENVIRONMENT ANALYSIS

Since power line monitoring using a drone actually belongs to aerial inspection, this section will first go over restrictions of aerial inspection with manned helicopters employed in Korea. Next, it will review how a high voltage of live-line state can have an impact on a drone through a series of experiments.

2.1 | Aerial inspection on manned helicopters (Lee, 2017)

Aerial inspection is referred to as diagnosis work to pick up abnormalities of transmission lines and check nearby locations



Voltage	\textcircled{X}	\textcircled{Y}
154 kV	20m	15m
345 kV	20m	20m
765 kV	40m	40m

FIGURE 1 Safe separation distance for aerial inspection
(\textcircled{X} : distance horizontally from the upper power line, \textcircled{Y} : distance vertically from the upper power line)

thoroughly, and to identify faults in the connection parts of power lines by using the helicopter with a thermal camera so that a possible power disconnection can be prevented. To do this job, safe separation distances are described as Figure 1.

Suspension conditions for aerial inspection are as follows:

- Wind speed is faster than 10 m/s.
- Visibility is within 1,000 m.
- The cloud height is within 304.8 m (1,000 ft) above the terrain.
- The facility/utility operation head or flight pilot decides to discontinue flight due to worsening weather conditions such as snow, rain, or fog, and so forth.
- The inspectors decide that they cannot monitor overheating coming from connection parts of power lines due to rising ground temperature.

2.2 | Analysis on EMI effects

Table 1 summarizes factors that may have an impact on hot-line work from the perspective of electrical environment. This shows that the electric field is generated by voltage and the magnetic field is produced by electric current. It also explains the corona causes audible noise and interferences in radio and TV reception. This subsection will examine how changes in the two continuous environmental factors of the electric and the magnetic fields affect drones.

First, to validate the impact of the electric field generated by voltage on the drones, a live-line flight test was executed in an indoor energized facility by using a small drone. Under the test, 345 kV was energized on the suspension insulator strings. During the live-line state, the experiment is designed to figure out (a) the closest distance the drone can approach; (b) safety when the drone contacts the ground side and; and (c) safety when the drone touches the energized line (Figure 2).

The test shows that when a drone flew very close to a high-voltage line or contacted an insulator located near the energized line, it worked normally. This explains that changes in the electric field would not have any impact on a drone movement. However, when the drone contacted the high-voltage line directly, it caused flashover failing a remote control function and leading the drone to go down. This result is consistent with that of the electrical

TABLE 1 Factors relevant to electrical environment of power lines (Kim, 2016)

Item	Voltage	Current	Height	No. of Sub-Cond.	Status of Surface
Electric Field	O		O		
Magnetic Field		O	O		
Audible Noise	O		O	O	O
Radio Interference	O		O	O	O
TV Interference	O		O	O	O

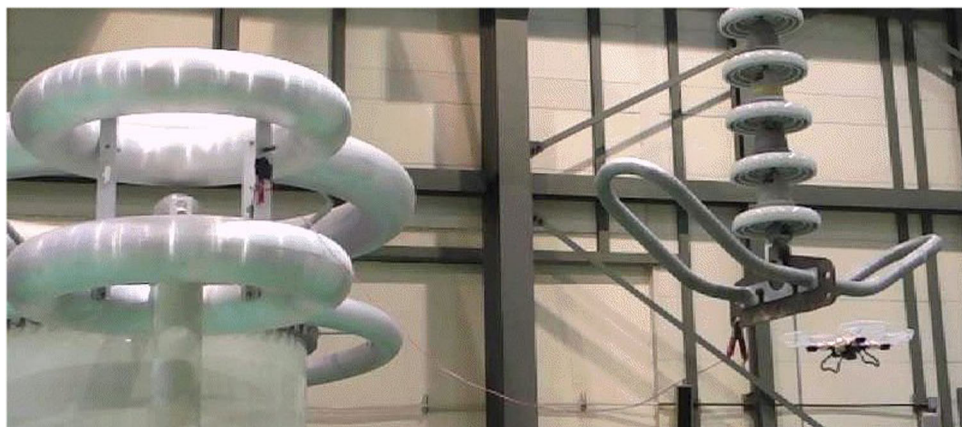
↓
Caused by “Corona”

effects testing conducted by EPRI (Unmanned Aircraft Systems Functional Specification for Local Structure Inspection, 2017). EPRI reported that the electric field, the magnetic field, the corona, and the arc in the power transmission lines did not affect a working drone but the drone's sensors could work abnormally when the drone contacted a high-voltage line directly. As will be described below, unlike the EPRI report, it was concluded that changes in the magnetic field did have an impact on the drone movement based on its experiments. Through the tests mentioned above, as long as the drone does not contact a high-voltage power line directly, it is assumed that the drone's accessibility to power transmission utilities is safe from the electric field.

In the following, it is described how the magnetic field produced by the electric current would affect drones. Figure 3 shows a graph of the magnetic field strength by separation distance from 380 kV transmission lines reported by King Fahd University of Petroleum & Minerals (Bakhshwain, Shwehdi, Johar, & AL-Naim, 2003). As shown, a considerable amount of the magnetic field is produced near the power transmission lines against 50 μ T of the geomagnetic field strength, which is a criterion to measure flight direction of a drone. It is judged that such magnetic field strength can have a big

impact on the geomagnetic sensor, which is necessary to measure direction of a drone's flight. That is, a value of the direction measured by a changing magnetic field would have a big error, which may cause the drone to fly to a wrong direction in an autopilot mode. The worst scenario is that the drone may collide with utilities and fall down.

To verify how the magnetic interference affects a drone, a small drone was used to measure the interference on the power transmission lines as seen in Figure 4: The tests were carried out in the span between tower No. 15 and 16 of 345 kV Sinokcheon-Cheongyang T/L, and in the span between 25 and 26 of 765 kV Sinseosan-Sinanseong T/L, respectively. At each run of the tests, a take-off location was moved starting from outside toward the center of power lines by five meters, and a drone was flown vertically from the original place in a manual control mode considering a possible wrong estimation of the flight direction due to the magnetic field. For the 345-kV lines, the starting location was 40 m from the center of power lines and for the 765 kV lines, from 80 m. Then, the screen of the ground control station (GCS) was monitored to check if compass error messages were displayed on it to pick up the magnetic interference.

**FIGURE 2** Task environment analysis using small drones

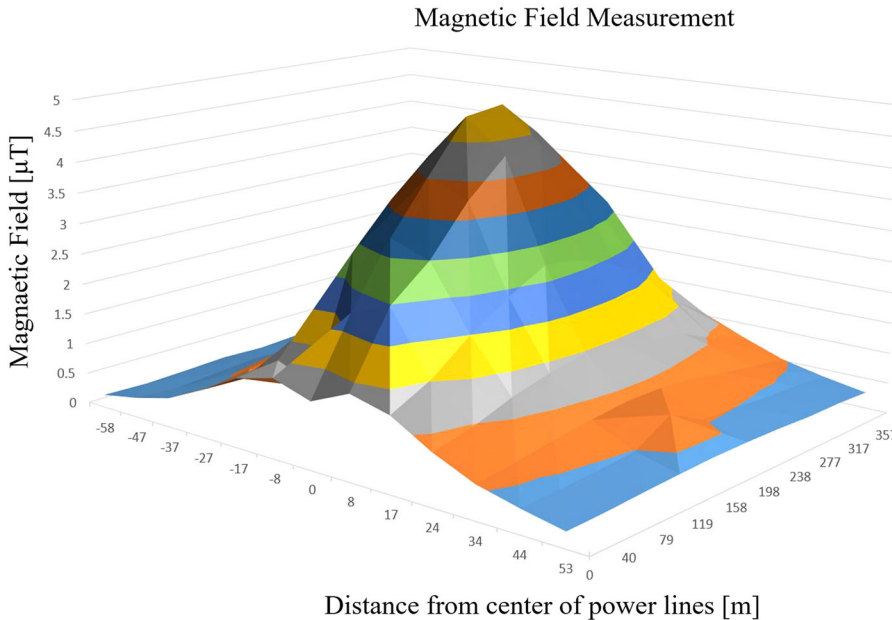


FIGURE 3 Magnetic field strength by separation distance from 380-kV power lines

As a test result, the GCS confirmed that the magnetic interference occurred when the drone flew within 15 m for the 345 kV and 30 m for the 765 kV from the center of the power lines. In order to identify how much the magnetic field changes, the magnetic field strengths were measured by flying the drone vertically at a separation distance of 12 m for 345 kV and at a separation distance of 25 m for 765 kV, respectively. As seen in Figures 5a,b, it was confirmed that actually $\pm 20\text{--}25\%$ of the volume of the magnetic field was produced against the geomagnetic field of 50 μT . Based on the tests reviewed, safe flight distances, where autopilot drones can fly without the magnetic field interference, were determined as 30 m for the 345 kV power lines and as 45 m for the 765 kV power lines in consideration of a safe margin of 15 m. This safe margin was empirically determined for a drone operator to respond to emergencies in which there occurs an unexpected problem in the drones or a sudden gust of wind.

3 | OPERATION METHOD OF AUTOPILOT INSPECTION DRONE

3.1 | Overall process

Figure 6 outlines a concept of the drone-based autopilot inspection for the power transmission lines in consideration of the safe flight distance without magnetic field interference. In this figure, the curved surfaces in various colors between steel towers represent the magnetic field strength produced on the 380 kV lines by location close to the power lines as shown in Figure 3. According to the concept of Figure 6, locations at a safe flight distance from the centers of the steel towers are supposed to be measured by a GPS co-ordinate measuring device. As opposed to how it appears in this figure, however, a location at a safe flight distance is actually calculated after the steel tower-based GPS co-ordinate are

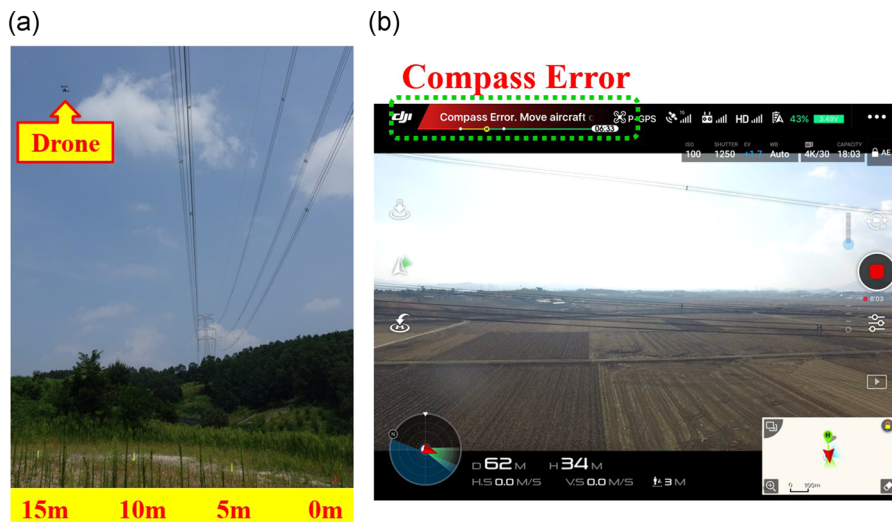


FIGURE 4 Magnetic field interference test by separation distance

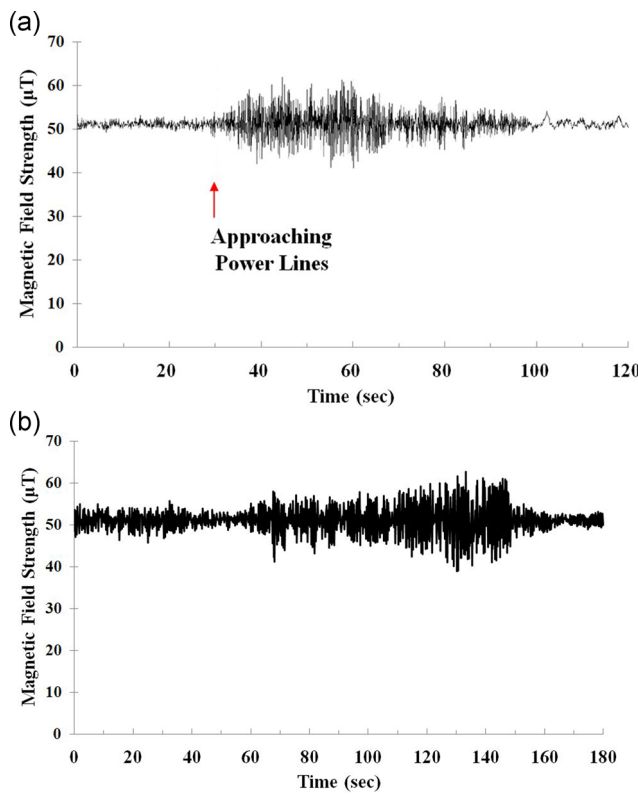


FIGURE 5 Measured data on magnetic field strength in the power transmission lines (a) 345kV (b) 765kV

measured. The inspection process is described in Figure 7. Each step is as follows:

3.2 | Measuring GPS co-ordinates of steel towers

Steel tower-based GPS co-ordinates must be calculated super-precisely because they are fundamental to the drone autopilot path. Many research papers have concluded that high-voltage

power lines would not have an impact on GPS signal reception (Rabah & El-Hattab, 2011; Silva & Olsen, 2002). Nonetheless, when the GPS co-ordinates at the center of a transmission tower were actually measured with a GPS co-ordinates measuring device, a location at some distance away from the tower center was often picked up, not the exact one. This tendency appeared more often on a transmission tower with a pole-type structure rather than with a lattice-type one, which is more widely used. These measurement errors are estimated to result from GPS signal distortion in the steel frame structure or at an area nearby steel poles. To avoid such a distortion, we adopted the following method to obtain the GPS co-ordinates of a tower as shown in Figure 8.

1. Measure GPS co-ordinates p_1, p_2, p_3 , and p_4 at the four corners of the tower foundation, respectively, instead of directly measuring the center of the tower.
2. Calculate the GPS co-ordinates P_C of the tower by averaging p_1, p_2, p_3 , and p_4 : $P_C = (p_1 + p_2 + p_3 + p_4)/4$.

Using the method of obtaining the geometrical center of the steel tower mentioned above, it is possible to obtain GPS co-ordinates for the steel tower that is very precise compared to the co-ordinate obtained through the traditional measuring method. Nonetheless, it has been observed that measuring values of one point among four measuring points sometimes deviate significantly from the actual location due to GPS signal interference by the steel tower structures or geographic features. To address this scenario, a new algorithm has been developed, which uses co-ordinates of the remaining three points well measured to correct the co-ordinates of the corresponding point instead of measuring the GPS co-ordinates of the corresponding point again in order to increase the efficiency of the task.

Figure 9 shows a procedure of the developed algorithm being applied when the measured GPS co-ordinates of one point among four corners of the steel tower base deviate from the allowed range. Here, $C(x_r, y_r)$ are actual center co-ordinates of the steel tower, l is the length of the tower foundation, $P_{Ci}(x_{Ci}, y_{Ci})$ are estimating values of the center co-ordinates of the steel tower to be obtained as the i th iteration of the algorithm proceeds, p_1, p_2, p_3 , and p_4 are GPS co-ordinate values to be measured near the four corners of the steel tower base, and $l_{i,i+1}$ indicates the distance between two measuring points. The algorithm developed for estimating the center GPS co-ordinates of the steel tower is as follows.

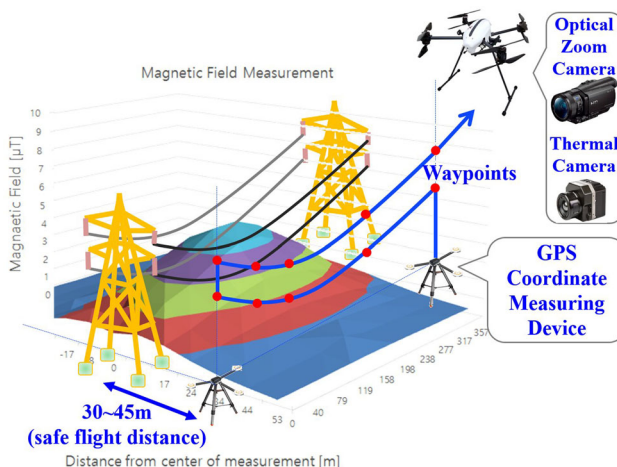


FIGURE 6 Concept on automatic drone inspection system for the transmission lines

1. First, an error-determining coefficient α is introduced to determine whether the measured co-ordinates deviate significantly from the actual location. For example, when a point p_2 deviates significantly from the allowance range as shown in Figure 9, two sides l_{12}, l_{23} in black lines are larger than αl to satisfy (1) below, so that the point p_2 may be determined as co-ordinate data deviating from the allowed range. Here, the coefficient α was set to 1.1 through simulations and its on-site verifications.

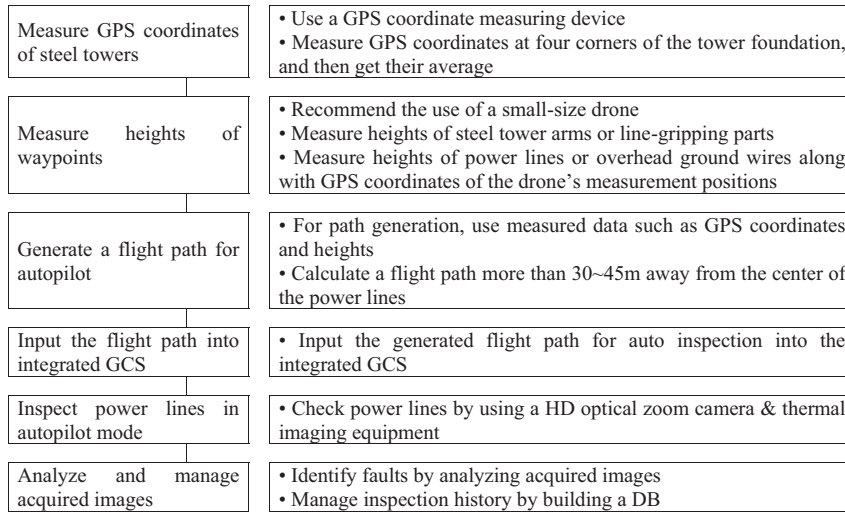


FIGURE 7 Automatic drone inspection process for transmission lines

$$l_{12} > \alpha l \text{ and } l_{23} > \alpha l \text{ and } l_{34} \leq \alpha l \text{ and } l_{41} \leq \alpha l \quad (1)$$

2. When the measured data p_2 is determined to deviate significantly from the actual location, p_2 isn't measured again, but is replaced with P_{C_1} to be calculated from (2) below.

$$\begin{aligned} P_{C_1} &= (x_{C_1}, y_{C_1}), \quad x_{C_1} = \frac{x_1 + x_2 + x_3 + x_4}{4}, \\ y_{C_1} &= \frac{y_1 + y_2 + y_3 + y_4}{4}. \end{aligned} \quad (2)$$

3. The two sides l_{1C_1} and l_{C_13} are calculated from the replaced P_{C_1} .

$$l_{1C_1} = \sqrt{(x_1 - x_{C_1})^2 + (y_1 - y_{C_1})^2} \quad (3)$$

$$l_{C_13} = \sqrt{(x_{C_1} - x_3)^2 + (y_{C_1} - y_3)^2} \quad (4)$$

4. The two sides l_{1C_1} and l_{C_13} are compared with αl to determine whether P_{C_1} deviates from the allowed range.

$$l_{1C_1} > \alpha l \text{ and } l_{C_13} > \alpha l \text{ and } l_{34} \leq \alpha l \text{ and } l_{41} \leq \alpha l \quad (5)$$

5. When P_{C_1} satisfies (5), P_{C_1} is, in turn, replaced with P_{C_2} to be calculated by (6).

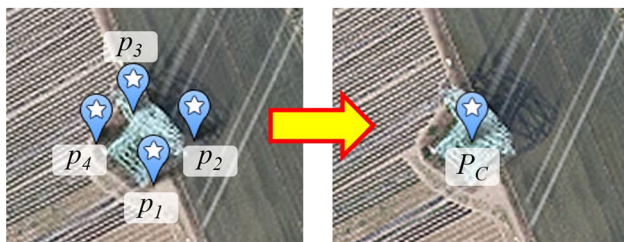


FIGURE 8 Calculation of geometric center co-ordinates from GPS co-ordinates measured at four corners of tower foundation

$$\begin{aligned} P_{C_2} &= (x_{C_2}, y_{C_2}), \quad x_{C_2} = \frac{x_1 + x_2 + x_3 + x_4}{4}, \\ y_{C_2} &= \frac{y_1 + y_2 + y_3 + y_4}{4} \end{aligned} \quad (6)$$

6. The two sides l_{1C_2} and l_{C_23} are calculated from the replaced P_{C_2} , and compared with αl again.
7. If the replacement procedure and comparison procedure above are repeated n times until the calculated two sides l_{1C_i} and l_{C_i3} all are less than or equal to αl , it is finally possible to obtain GPS co-ordinates P_{C_n} to be converged to the center of the steel tower.

Because site conditions for the tasks of measuring the steel towers were substantially poor in many cases and the task of measuring each GPS co-ordinate took a lot of time, the developed algorithm has been applied very usefully in the sites. Please refer to Kim, Park, Lee, Choi, and Ham (2017) for detailed information on the GPS co-ordinate-measuring algorithm for a transmission tower.

3.3 | Measuring heights of waypoints

The power facilities to be inspected by drones consist of two main parts: steel tower (insulator, fittings included) and power lines.

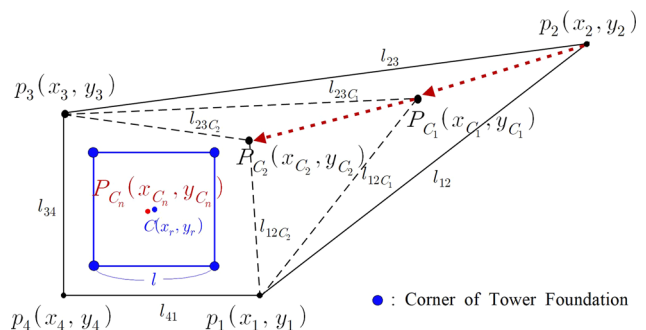


FIGURE 9 A procedure of applying the correction algorithm when the GPS co-ordinate of one point deviates from the allowed range

Since the steel towers' GPS co-ordinates were determined, the next step is to gain the relevant height data and the use of a small-size drone is recommended. For a tension-type tower, heights of its arms have to be measured, and for a suspension-type tower, heights of line-gripping parts have to be done. The power lines, whose components include upper phase, middle phase, lower phase conductors, and overhead ground wires, hang down from the end of the steel tower arms. To secure data of intermediate waypoints, the small-size drone is flown at the height of the hung power line, and measure heights of power lines along with GPS co-ordinates of the drone's measurement positions. Usually, spacer dampers installed on the power line or aerial balls installed on the overhead ground wire are measured. If there is no attachment, the span between the towers has to be divided equally to measure power line data at the relevant location.

3.4 | Generating autopilot flight path

An autopilot flight path of a drone is generated as follows on the basis of GPS co-ordinates and height data acquired during the previous steps:

1. Calculate the starting point and the end point of the flight path at a safe flight distance from the center A and B of the steel towers, respectively.
2. Determine a drone's direction to monitor power lines by calculating the direction perpendicular to the span between the two towers.
3. The measurement locations to get power line data in the previous step are not the one based on the safe flight distance but on a random position of the drone manually controlled by a pilot. Accordingly, you need to convert GPS co-ordinates of the measurement locations into waypoints based on the safe flight distance as shown in Figure 10.

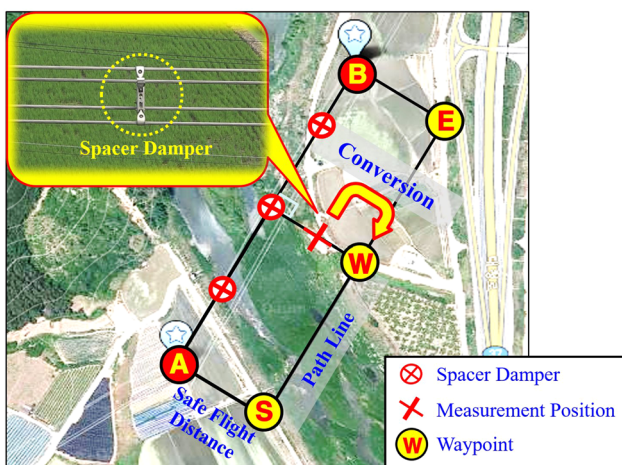


FIGURE 10 Calculation of starting and end points of flight path and drone direction; generating waypoints for power line inspection based on safe flight distance

As mentioned in Section 3.3, the transmission lines include upper phase, middle phase, lower phase conductors, and overhead ground wires. To construct intermediate waypoints between two towers for the autopilot flight path, all the related heights of the hung power lines should be measured. Next, measuring all height data associated with "upper phase, middle phase, lower phase conductors, and overhead ground wires" in sites with poor accessibility may take a lot of time. For this reason, we developed a new path-generating method based on the geometric relation that three-phase conductors have the approximately same sags and spans as each other. This method can generate flight path data of the remaining conductors by only measuring height data associated with the upper phase conductor, and by obtaining a curve equation of the upper phase conductor considering the sag in order to increase the efficiency of the path generating task.

In the newly proposed flight path-generating method, considering that the transmission line is a type of catenary line, a curve equation for the upper phase conductor is obtained through the procedure described below.

Assuming that the lowest point of the transmission line due to sag is an original point, the transmission line is a type of catenary line, so that an altitude of the transmission line y forms a catenary line equation of (7) with a span distance being in an x axis (Sag design standard for overhead transmission lines, 2013).

$$y = p \left\{ \cosh \left(\frac{x}{p} \right) - 1 \right\} = p \left(\frac{e^{\frac{x}{p}} + e^{-\frac{x}{p}}}{2} - 1 \right). \quad (7)$$

When the catenary line equation above is transformed into Taylor series, (8) is obtained.

$$y = \frac{1}{2} p \left[\left\{ 1 + \frac{x}{p} + \frac{1}{2!} \left(\frac{x}{p} \right)^2 + \dots \right\} + \left\{ 1 + \left(-\frac{x}{p} \right) + \frac{1}{2!} \left(-\frac{x}{p} \right)^2 + \dots \right\} - 2 \right] = p \left(\frac{1}{2!} \left(\frac{x}{p} \right)^2 + \frac{1}{4!} \left(\frac{x}{p} \right)^4 + \frac{1}{6!} \left(\frac{x}{p} \right)^6 + \dots \right). \quad (8)$$

When sag parameter p is obtained for the catenary line in (8), results with a high level of precision can be obtained, as it comprises high order terms a lot, but for simplicity, the catenary line equation was approximated only using a quadratic term, as follows.

$$y \approx x^2 / 2p. \quad (9)$$

Here, a coefficient of the quadratic term, $1/2p$, may be obtained through a regression analysis for the altitude data of the upper phase conductor to be measured. To describe how to determine $1/2p$ in detail, waypoints data measured from a upper phase conductor are given as an example in Table 2.

As mentioned before in Figure 10, the measurement locations in Table 2 are converted into waypoints based on the safe flight distance, and then converted again into the co-ordinates on the x' and y' axes of Figure 11, which finally results in Table 3.

TABLE 2 Waypoints example measured at upper phase conductor

Location	Latitude	Longitude	Height (m)
Tower A	36.8187	126.9350	51.0
1	36.8188	126.9352	45.1
2	36.8191	126.9355	41.0
3	36.8194	126.9360	36.8
4	36.8197	126.9365	30.4
5	36.8201	126.9370	30.5
6	36.8205	126.9376	35.2
7	36.8208	126.9380	40.0
Tower B	36.8211	126.9384	46.3

These co-ordinate points can be approximated into a second-order polynomial of (10) by using the polynomial least square approximation method as shown in Figure 12.

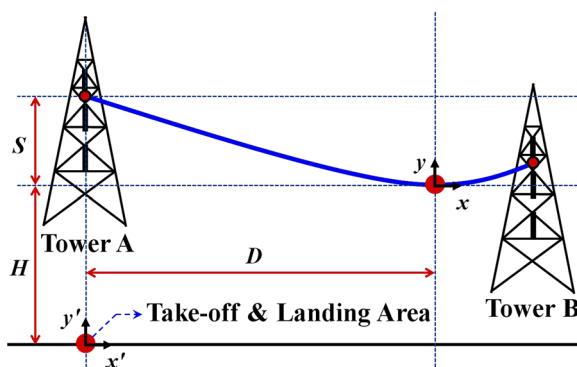
$$y \approx 0.0004x^2 - 0.1834x + 51.0922. \quad (10)$$

This equation is easily converted into the equation of $y = 0.0004x^2$ on the x and y axes of Figure 11, and consequently, p is obtained from the comparison of its coefficient with that of (9) as follows: $0.0004 = 1/2p$. When sag parameter p obtained through the procedure above is substituted into (7), it can result in obtaining the catenary line equation.

However, the finally obtained catenary line equation has the lowest point of the transmission line according to the sag as the original point, so that the original point must be moved to the location of a take-off and landing area in order to utilize the catenary line equation for generating the flight path. The catenary line equation may be arranged as the equation shown below with regard to x from (7) in order to obtain the horizontal distance D between steel tower A and the lowest point of the transmission line.

$$x = p \times \ln \left\{ \left(\frac{y}{p} + 1 \right) \pm \sqrt{\left(\frac{y}{p} + 1 \right)^2 - 1} \right\}. \quad (11)$$

D may be obtained as follows from (11).

**FIGURE 11** Calculation of a flight path point using a catenary line equation**TABLE 3** Converted co-ordinate points to obtain catenary line equation

Location	x' axis (distance, m)	y' axis (height, m)
Tower A	0.0	51.0
1	31.8	45.1
2	66.8	41.0
3	121.5	36.8
4	183.0	30.4
5	238.7	30.5
6	307.2	35.2
7	361.2	40.0
Tower B	408.1	46.3

$$D = p \times \ln \left\{ \left(\frac{S}{p} + 1 \right) \pm \sqrt{\left(\frac{S}{p} + 1 \right)^2 - 1} \right\}, \quad (12)$$

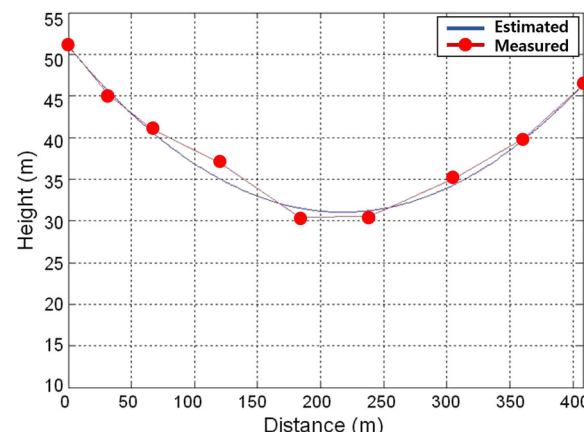
where S denotes the height difference the transmission line hangs down according to the sag.

A reference co-ordinate system (x' , y') in generating a flight path of the drone has the take-off and landing area of the drone as its original point, so that as shown in Figure 11, the reference co-ordinate system must be moved by horizontal distance D and vertical distance H from the transmission line lowest point co-ordinate system (x , y). Accordingly, an equation for generating the flight path may finally be obtained as follows.

$$y' = p \left\{ \cosh \left(\frac{x' - D}{p} \right) - 1 \right\} + H. \quad (13)$$

3.5 | Inputting flight path into integrated ground control station

Waypoints created on the previous steps for the automated drone inspection are entered into integrated GCS, and the final confirmation is made on the input waypoints displayed in 3D on the screen. If

**FIGURE 12** Converted waypoints on the x' and y' axes, and their approximation by curve fitting

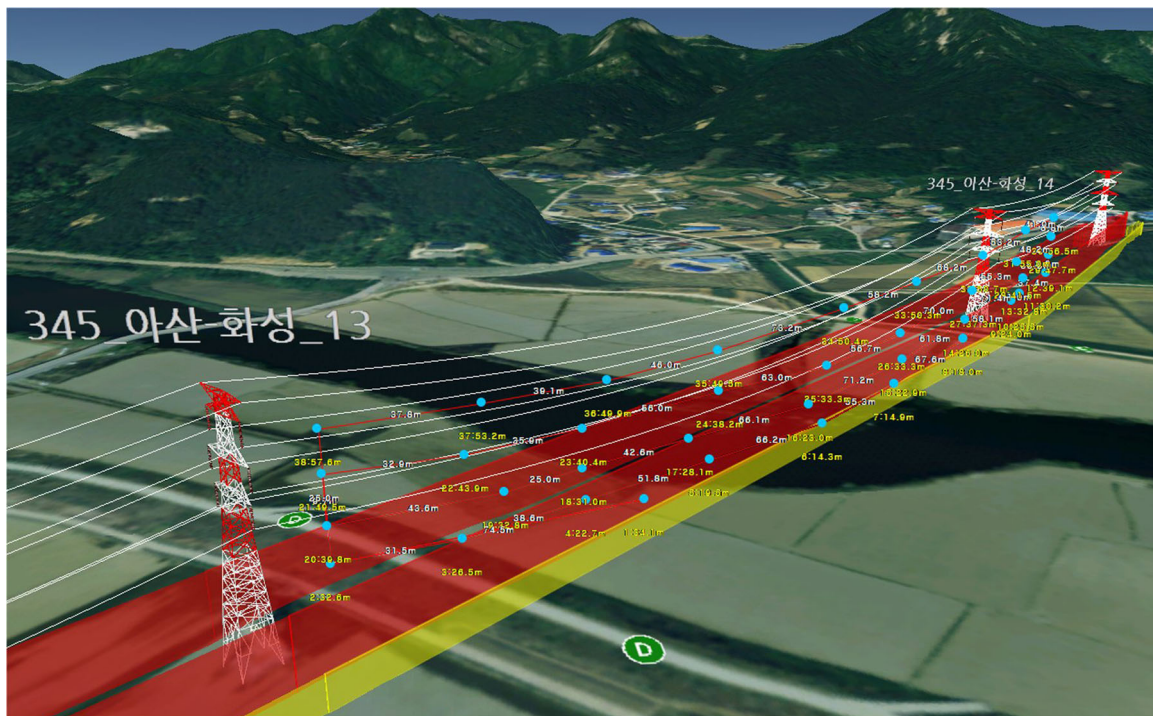


FIGURE 13 Example of autopilot flight path in integrated ground control station

needed, each waypoint is edited. Especially, you must make sure that the input flight path stays outside of the magnetic fence (yellow color denotes caution, and red, danger), which represents the magnetic field interference (Figure 13).

3.6 | Inspecting power lines and analyzing results

The minimum number of human operators assigned to the automatic drone inspection for power transmission lines includes one person for the integrated GCS and one for the camera gimbal control. It would be desirable to deploy one on-site manager for better work efficiency. The drone executes its inspection in autopilot mode with the predetermined path given by the GCS. On the contrast, the camera gimbal is remotely controlled by an operator in order to track and capture power lines. HD images and thermal images gained during the flight will be stored in the SD card and used later to identify faults through image analysis.

4 | FIELD TESTS

4.1 | Drone system

It is not that hard to find drones with specifications qualified for transmission line inspection because of advanced drone technology and various commercial drones. However, their GCSs are quite different depending on manufacturers, which power utility operators found difficult to use. Not only that, the two-dimensional satellite map provided by commercial GCSs does not display power transmission lines appropriately and is not able to express

waypoints of a drone and its current location in 3D. Accordingly, it would be difficult for a pilot in a remote place to identify actual situation of the flying drone. To cope with these practical problems, our research institute newly developed an integrated GCS for power line inspection, which is able to interconnect and control any commercial drones installing DJI A3, a stable FC (flight controller) and widely used onto most commercial drones. Figure 14 shows a configuration of a drone-based automatic inspection system with the integrated GCS dedicated to the power transmission lines.

Table 4 shows the minimum drone specifications for the transmission line inspection that were recommended through frame review of different drones and field tests. An HD optical zoom

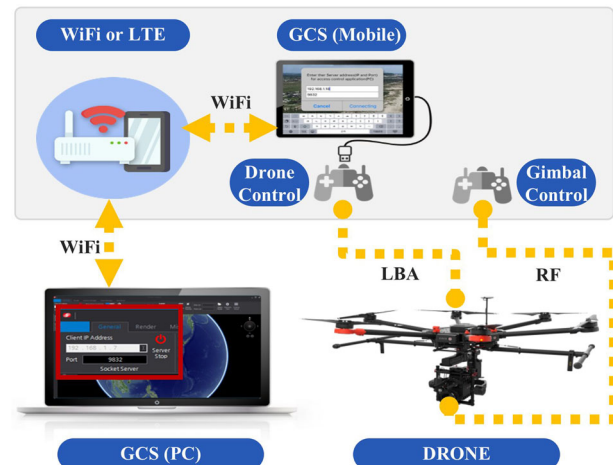


FIGURE 14 Configuration of automatic drone inspection system

TABLE 4 Minimum specifications of power line inspection drone

Items	Description	Remarks
Weight	Below 12 kg recommended	With batteries
Payload	5 kg or more	
Flight controller	DJI A3	Compatible with integrated GCS
Max wind resistance	8 m/s or more	
Hovering accuracy	Vertical ± 0.5 m, Horizontal ± 1.5 m	P-Mode, GPS
Battery spec	A total amount of over 20,000 mAh recommended	
Flight time	Minimum 30 min or longer	No payload
Operating temperature	-10 to 40°C recommended	
Built-in equipment	Optical zoom camera ^a , thermal imaging camera	
Others	<ul style="list-style-type: none"> * Independent control of camera gimbal * Image display in real-time * Retractable landing gear recommended * Return-to-Home/Failsafe mode * SDK support 	

Abbreviation: GCS, ground control station.

^aPossible to inspect at the separation distance of 30 to 45 m from the center of the power line.

camera and a thermal imaging camera to be built onto the drone were chosen through image quality tests so that the drone can keep at the distance of 30–45 meters away from the transmission lines and inspect overhead power utility facilities. All images taken during the inspection are sent to operators in real-time so that they can check directly in the field. Also, these images are stored separately and used to identify faults through a precise diagnosis in the office later. Main functions of the integrated GCS are summarized in Table 5.

4.2 | Field test results

From June to July in 2017, our institute applied its newly developed automatic drone inspection technology to 31 steel towers under the request of Transmission & Substation Operation Department of KEPCO. Figure 15 shows a field test example of autopilot drone inspection including a desired flight path, its tracking result and tracking errors. Compared with the size of steel towers and the span between towers, the tracking errors mainly caused by GPS measurement errors are too small to affect the quality of the pictures that the drone takes by using an optical zoom camera and a thermal imaging camera. As a result, the new technology detected 32 faults—a split in a connection sleeve, three defective stockbridge dampers, four birdcaging conductors, eight damages in aerial balls, four birdcaging armor rods, three defects in construction, six bird's nests, a damaged ground wire and two unnecessary attachments. Figure 16 shows some examples of the detected faults. Especially, a split in a high-temperature connector sleeve may be caused by water inclusion and freezing, and can make the connector continue to degrade, eventually leading to its mechanical failure. As seen in Table 6, the target power lines for the pilot test included areas where humans find it difficult to inspect due to mountainous topography and rivers. Thus, the test could identify practical problems that may

arise from different working conditions. This chapter will review possible issues when the drone works in the field and suggest measures to solve them.

4.2.1 | Selecting take-off & landing areas

Generally, the safe landing area for UAV should have at least two features: a flat surface and its size big enough for UAV's dimension and movement (Cesetti, Frontoni, Mancini, Zingaretti, & Longhi, 2010; Li, 2013). Another condition for the landing area is the place where target power lines should be within visual line-of-sight of a drone operator according to the related regulations.

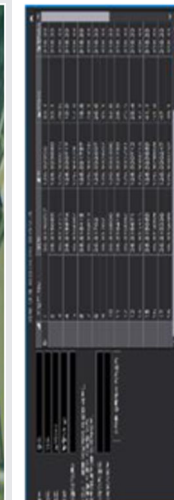
Since AC double-circuits power lines are typically used for power transmission in Korea, each circuit has to be inspected by a drone separately, and therefore, for accessible power lines in the flatland, a landing area to meet the requirements above is designated for each circuit, respectively, as in the example of Figure 17.

However, in the case of power lines where steel towers are located along mountain slopes, a take-off and a landing area could be selected for one circuit only as seen in Figure 18, but it was impossible to pick the area for the other circuit because of no accessibility in mountainous terrain.

4.2.2 | How to operate drones in mountainous topography

As mentioned above, transmission lines located on mountain slopes are not usually approachable for the drone inspection with the existing method for landing area selection because steel towers can be reached only from one side. To solve this issue, a new approach was proposed with which, the drone was started off from the accessible side and was moved over the upper power line or under the lower power line to monitor the other side. However, there is one

TABLE 5 Major functions of integrated GCS

Functions	Graphic Description	Functions	Graphic description
Drone monitoring		Path planning & flight simulation	
3D mapping (towers, power lines, geomagnetic fences)		Autopilot flight control	
Mission management		Image data management	
Abbreviation: GCS, ground control station.			

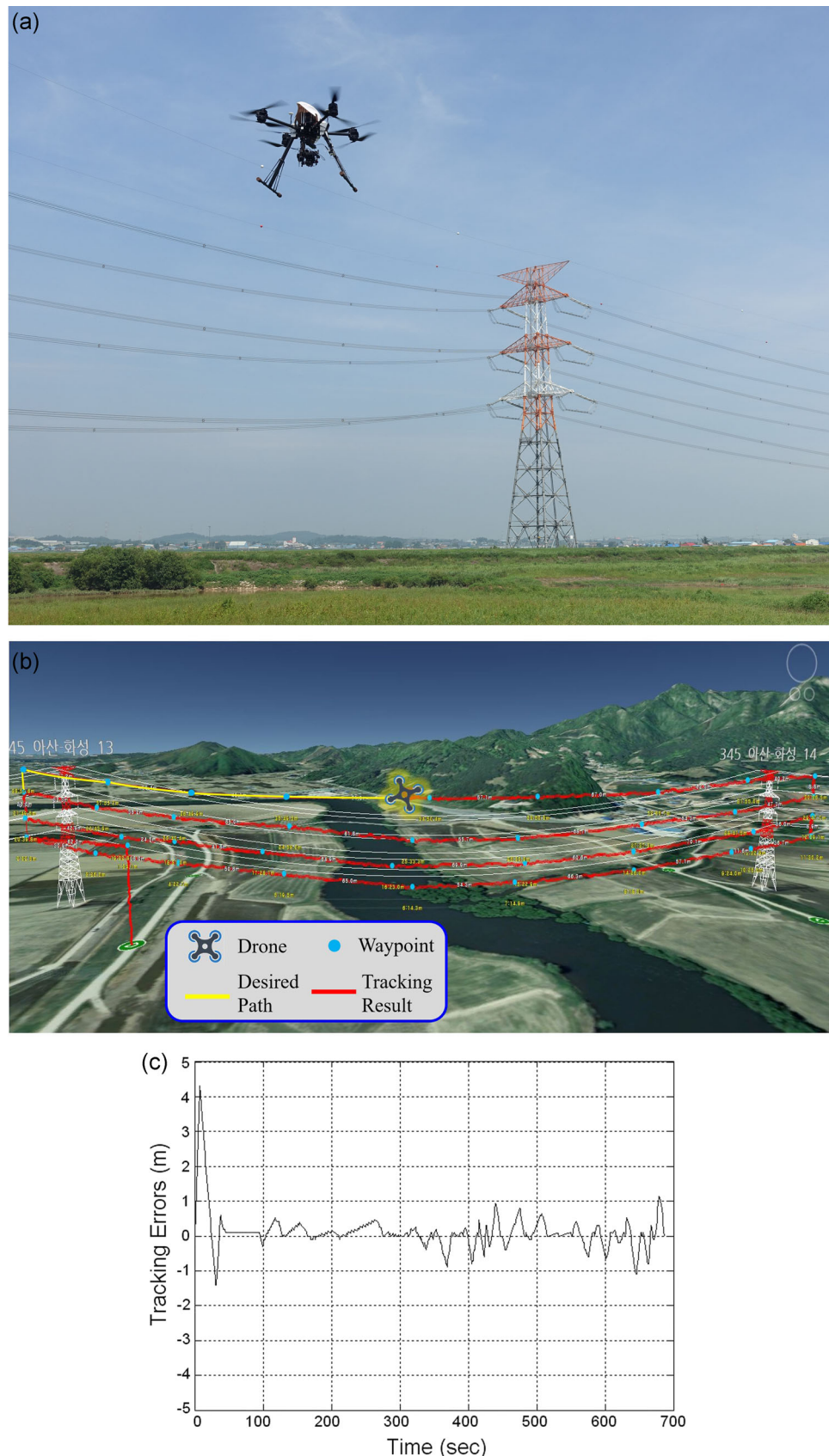


FIGURE 15 Example of autopilot drone inspection on power transmission lines (a) Autopilot drone inspection (b) Desired flight path and its tracking result (c) Tracking errors in altitude



FIGURE 16 Examples of detected faults

condition: when the drone crosses the power line, its flight must be higher or lower than the safe flight distance from the power lines (30 m for lower than 345 kV, 45 m for 765 kV) for operation (Figure 19).

Even though the span is accessible from both sides, you can still adopt this new method to inspect both circuits. It means that the movement between two landing areas can be reduced and work efficiency can be increased. For instance, the steel towers of No. 24-27 in the 154 kV Asan-Yesan T/L could be monitored from the same landing area without movement between the spans as shown in Figure 18.

4.2.3 | Flight path generating process in mountain areas

The flight path for automatic inspection includes four steps at a safe flight distance from the center of the lines: (a) lower power line → (b) middle power line → (c) upper power line → (d) overhead ground wire. Unfortunately, this four-step process path can be worrisome with steel towers located on mountain slopes because the normal path would make the drone clash with trees.

In the example of Figure 20, it was checked in advance with a small-size drone whether an inspection drone may collide with trees or not, and it was concluded that if the flight path had been changed to (middle power line [videotaping the lower power line from the middle power line path] → middle power line → upper power line → overhead ground wire) instead of the normal path, the drone would not clash with trees even though they looked

close. As the inspection drone was actually tried in auto mode, it hit the trees while flying at a height of the middle power line as Figure 20. A follow-up analysis suggested that an optical illusion might be caused by carelessly controlling a camera gimbal of the small drone during the flight. That was why the trees seemed located lower than the actual position.

To avoid such a collision in the mountainous areas, installing an obstacle detection sensor onto the drone may be considered. Considering fast flight speed of a drone, irregular height and distribution of trees, it would be desirable to create a flight path which doesn't hit the trees from the viewpoint of ensuring flight safety. Based on the tests above, our institute defined a process that executes a preliminary flight first as below to check whether the drone collides with trees during its inspection in mountainous areas (Figure 21).

1. Examine steel towers in mountainous areas and decide the minimum height for inspection (for safe flight, define enough height greater than height of nearby trees among the heights of the lower, middle, upper power lines and overhead ground wire).
2. Generate a flight path to monitor all steel towers in the area while maintaining the minimum height for inspection.
3. Fly the drone on autopilot along the generated path at the flight speed of 1 m/s and check whether it collides with trees (1 m/s was defined based on the field experiences).
4. If there is a possibility of collision, stop the flight and return.
5. By increasing the minimum inspection altitude higher, repeat steps 2-4 until the drone does not collide with trees in all spans.

TABLE 6 Target power lines and inspection results

Voltage	Test sites	Range (tower No)	Topography	No. of defects
765 kV	Shinseosan-Shinanseong	34-38	Farmland, river crossing	6
345 kV	Asan-Hwaseong	11-15	Farmland, river crossing	4
	Shingimhae-Samchunpo	31-40	Mountainous area	15
154 kV	Asan-Yesan	23-27	Mountainous area	3
	Shingoseong-Tongyeong	60-65	Mountainous area, farmland	4

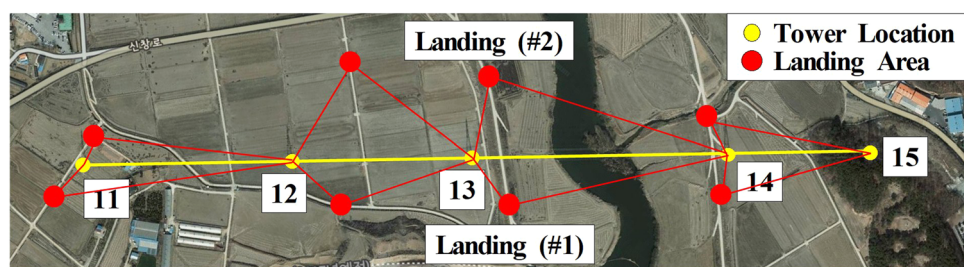


FIGURE 17 Landing area selection in flat area (345 kV Asan-Hwaseong T/L)

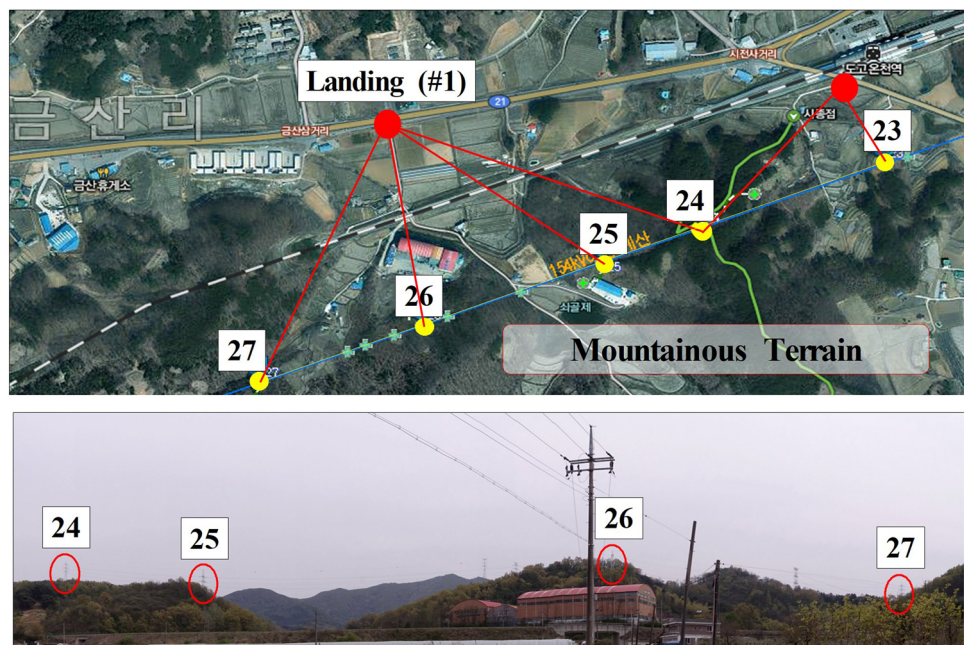


FIGURE 18 View from take-off and landing area in mountainous terrain (154 kV Asan-Yesan T/L No.24~27; all towers within visibility)

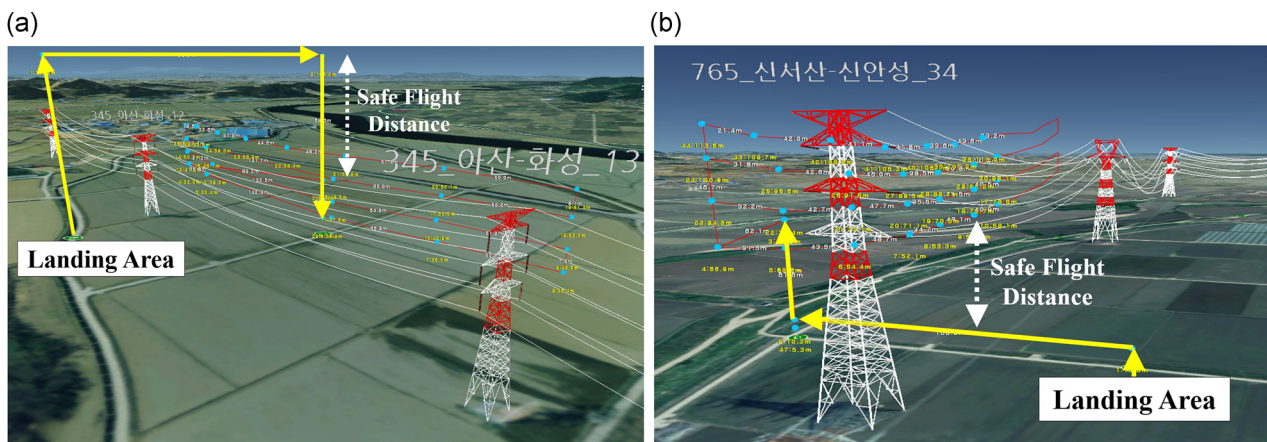


FIGURE 19 Opposite side inspection crossing power lines (a) Over the upper line (b) Under the lower line

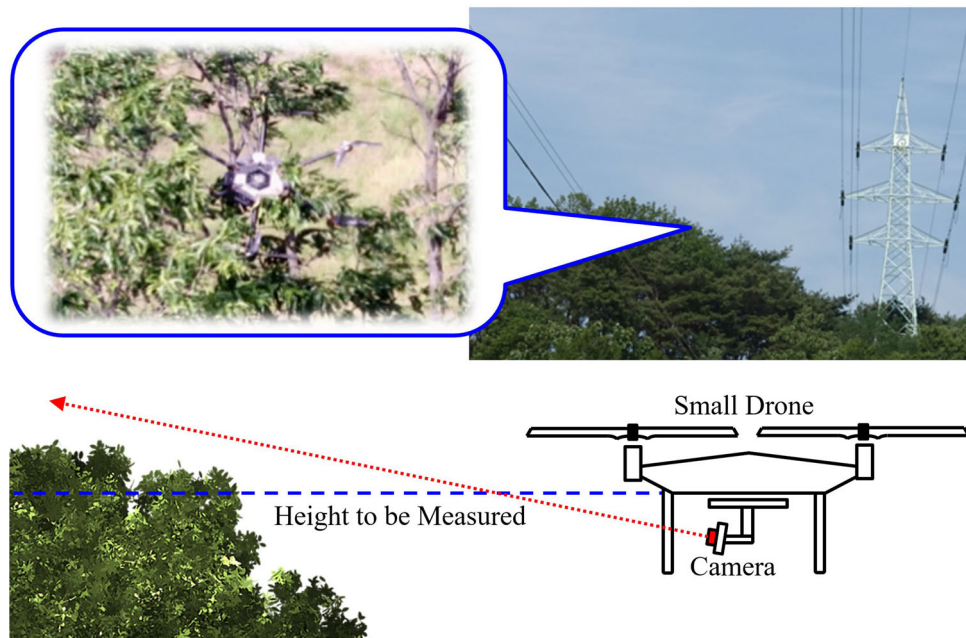


FIGURE 20 Example of drone crash with trees and its damage

Through the preliminary flight mentioned above, the starting altitude for the automatic drone inspection was set up as the minimum height where the drone never collides with trees. It is possible to increase the altitude in some sections for drone collision avoidance.

The reason that the drone can inspect the target at a much higher altitude than the target height is: the drone flies keeping at a safe flight distance 30–45 m away from the center of the transmission lines. As seen in Figure 22, it is possible to videotape the lowest power line due to enough separation distance from power lines, even

though you define the minimum height for inspection greater than the original one or you fly the drone at the height of the overhead ground wire.

5 | CONCLUSION

Drones have been limitedly used by pilots in manual mode to inspect power transmission lines. Even professional drone pilots are often



FIGURE 21 Example of preliminary flight path to check drone collision with trees

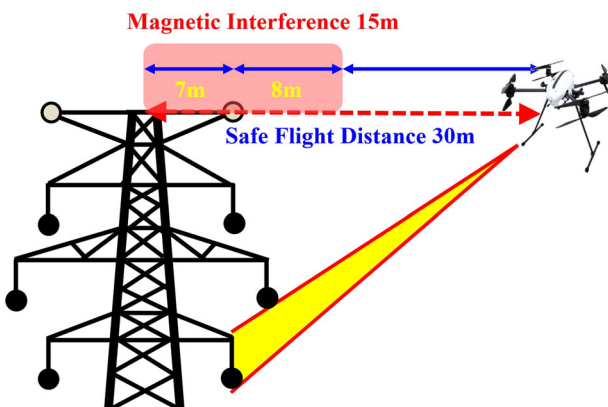


FIGURE 22 Videotaping the lower power line at the height of ground wire

reluctant to undertake this study, however, because it is widely known that an invisible interference is exerted on a drone near ultrahigh voltage power lines, and a small driving mistake may have huge ramifications. This paper is the first to provide an operational guideline for using an autopilot drone to monitor power transmission lines in an easier and more organized manner. The new methods of measuring GPS co-ordinates of a steel tower and planning a drone flight path for power line inspection were presented to overcome GPS signal distortion and magnetic interference near live power lines, respectively. In addition, some effective solutions were proposed to resolve practical operational issues in various environments which had been difficult to approach before, such as mountainous areas and rivers. The proposed operational approach was proven through a pilot test to be safe and efficient. If the drone operation technology is adopted widely for electric utilities in the future, it could contribute not only to maintaining the lines in a safe manner but also to creating an early market for 4th Industrial Revolution technologies.

ACKNOWLEDGMENTS

This paper presents the results of “Development of Deep Learning-based Automatic Diagnosis Drone System for Patrol and Inspection of Power Transmission Lines” project supported by 2016 Main R&D Projects performed by Korea Electric Power Corporation.

ORCID

Joon-Young Park  <http://orcid.org/0000-0003-3423-9389>

REFERENCES

- Bakhashwain, J. M., Shwehdi, M. H., Johar, U. M., & AL-Naim, A. A. (2003). Magnetic fields measurement and evaluation of EHV transmission lines in Saudi Arabia. In *Proceedings of the International Conference on Non-Ionizing Radiation at UNITEN*, Kuala Lumpur, Malaysia.
- Cesetti, A., Frontoni, E., Mancini, A., Zingaretti, P., & Longhi, S. (2010). A vision-based guidance system for UAV navigation and safe landing using natural landmarks. *Journal of Intelligent and Robotic Systems*, 57(1), 233–257.
- ComEd gets OK to deploy drones for power system inspections (2015). Retrieved October 1, 2019, from <https://www.eenews.net/stories/1060016677>
- Han, Y., Liu, Z., Lee, D. J., Liu, W., Chen, J., & Han, Z. (2018). Computer vision-based automatic rod-insulator defect detection in high-speed railway catenary system. *International Journal of Advanced Robotic Systems*, 15(3), 1–15.
- Kim, S. T., Park, J. Y., Lee, J. K., Choi, I. H., & Ham, J. W. (2017). Development of GPS coordinates measuring algorithm for a transmission tower. *KEPCO Journal on Electric Power and Energy*, 3(2), 99–105.
- Kim, Y. H. (2016). Design methods for eco-friendly overhead transmission line. *Career Development Education Program of KEPCO Research Institute*.
- Larrauri, J. I., Sorrosal, G., & González, M. (2013). Automatic system for overhead power line inspection using an unmanned aerial vehicle—RELIFO project. In *Proceedings of International Conference on Unmanned Aircraft Systems*, Atlanta, Georgia.
- Lee, J. H. (2017). *Operational standards for overhead power transmission lines (29th revision)*, Transmission & Substation Operation Department of KEPCO.
- Li, X. (2013). A software scheme for UAV's safe landing area discovery. *Proceedings of AASRI Conference on Intelligent Systems and Control*.
- Luque-Vega, L. F., Castillo-Toledo, B., & Loukianov, A. (2014). Power line inspection via an unmanned aerial system based on the quadrotor helicopter. *Proceedings of IEEE Mediterranean Electrotechnical Conference*.
- Martinez, C., Sampedro, C., Chauhan, A., Collumeau, J. F., & Campoy, P. (2018). The power line inspection software (PoLIS): A versatile system for automating power line inspection. *Engineering Applications of Artificial Intelligence*, 71, 293–314.
- Nguyen, V. N., Jenssen, R., & Roverso, D. (2018). Automatic autonomous vision-based power line inspection: A review of current status and the potential role of deep learning. *International Journal of Electrical Power & Energy Systems*, 99, 107–120.
- On Airborne Inspections: Aircraft and Crews (2014), Newsletter of Albatroz Engineering, May-June 2014.
- PPL starts using drones to help inspect high-voltage lines (2015). Retrieved October 1, 2019, from https://lancasteronline.com/business/local_business/ppl-starts-using-drones-to-help-inspect-high-voltage-lines/article_4a326d68-7bd7-11e5-ae0f-8bf26645220b.html
- Rabah, M., & El-Hattab, A. (2011). Investigating the impact of high voltage power lines on GPS signal. *Zfv-Zeitschrift für Geodäsie, Geoinformation und Landmanagement*, 6, 338–343.
- Ribeiro, L. V., Duarte, C. S. F., Ramos, A. C. B., & Mora-Camino, F. (2018). Visual servo control in quadrotor for power line tracking. *Proceedings of 10th International Micro-Air Vehicles Conference*.
- Sag design standard for overhead transmission lines (DS-1211) (2013). Korea Electric Power Corporation.
- Silva, J. M., & Olsen, R. G. (2002). Use of global positioning system (GPS) receivers under power-line conductors. *IEEE Transactions on Power Delivery*, 17(4), 938–944.
- Unmanned Air Systems for Transmission Line Inspection: Phase 2 - Demonstrations of Local Structure Inspection of Energized Lines (2016). EPRI, Palo Alto, CA: 2016.3002008888.
- Unmanned Aircraft Systems for Power Line Inspection: Field Demonstrations and Vendor Profiles (2015). EPRI, Palo Alto, CA: 2015.3002005721.
- Unmanned Aircraft Systems Functional Specification for Local Structure Inspection: Including Electrical Effects Test Results (2017). EPRI, Palo Alto, CA: 2017.3002009589.

- Wang, B., Chen, X., Wang, Q., Liu, L., Zhang, H., & Li, B. (2010). Power line inspection with a flying robot. *Proceedings of International Conference on Applied Robotics for the Power Industry*.
- Wang, B., Han, L., Zhang, H., Wang, Q., & Li, B. (2009). A flying robotic system for power line corridor inspection. *Proceedings of IEEE International Conference on Robotics and Biomimetics*, Guilin, Guangxi, China.

How to cite this article: Park J-Y, Kim S-T, Lee J-K, Ham J-W, Oh K-Y. Method of operating a GIS-based autopilot drone to inspect ultrahigh voltage power lines and its field tests. *J Field Robotics*. 2019;1–17. <https://doi.org/10.1002/rob.21916>